Nucl. Phys. B 1004 (2024) 116564

Contents lists available at ScienceDirect

Nuclear Physics, Section B

journal homepage: www.elsevier.com/locate/nuclphysb

High Energy Physics – Phenomenology

Search for a leptoquark and vector-like lepton in a muon collider

Nivedita Ghosh [a,*], Santosh Kumar Rai [b], Tousik Samui [c]

[a] Centre for High Energy Physics, Indian Institute of Science, Bengaluru 560012, India
[b] Regional Centre for Accelerator-based Particle Physics, Harish-Chandra Research Institute, A CI of Homi Bhabha National Institute, Chhatnag Road, Jhunsi, Prayagraj – 211019, India
[c] Department of Physical Sciences, Indian Institute of Science Education and Research Kolkata, Mohanpur, 741246, India

ARTICLE INFO

Editor: Hong-Jian He

ABSTRACT

The proposal for a high-energy muon collider offers many opportunities in the search for physics beyond the Standard Model (BSM). The collider by construction is likely to be more sensitive to the muon-philic models, primarily motivated by the BSM explanation of muon $(g-2)$ excess and quark flavor anomalies. In this work, we explore the potential of the proposed muon collider in the context of such models and focus on one such model that extends the Standard Model (SM) with a leptoquark, a vector-like lepton, and a real scalar. In this model, we propose searches for TeV scale leptoquarks in $2\mu + 2b + \not{E}_T$ channel. Notably, the leptoquark can be produced singly at the muon collider with a large cross-section. We have shown that a significant signal in this channel can be detected at a 3 TeV muon collider even with an integrated luminosity as low as $\sim 10\ \text{fb}^{-1}$.

1. Introduction

In the high energy frontier, the highest energies have been achieved in the hadron colliders since the protons could be accelerated to much higher energies than the electrons. The Large Hadron Collider (LHC) has achieved an impressively high beam energy of 6.8 TeV for each colliding proton, making it the highest ever for any collider. The available hard scattering energy would be much more in a hadron machine compared to a machine containing electron or positron beams. The hadron machines, however are unable to use the full energy of the colliding protons due to their composite nature. Moreover, while having several advantages in the energy frontier, the hadron collider is plagued by a noisy environment in the form of unwanted hadronic activity and smearing effects from the parton distribution functions (PDFs), which compromises the precision studies. On the other hand, a much higher energy of the muon beams is achievable through a circular collider due to its significantly smaller synchrotron radiation compared to an electron beam. The muon, being an elementary particle, can, therefore, give high center-of-mass energies in the hard collisions with a very little energy spread due to the suppressed radiative effects of *bremsstrahlung* and *beamsstrahlung* [1,2]. This, in turn, helps in the precision measurement of observables and particle properties. Another interesting possibility at these very high-energy muon colliders would be the generation of electroweak gauge bosons as partons of the beam through collinear radiation. These will emerge as electroweak PDFs [3–6], that can have implications in the study of vector boson fusion (VBF) processes. It is for this reason that the muon collider is also advocated as a "VBF collider" [7]. So, to some extent, a muon collider combines the advantages of *pp* and *ee* colliders, *i.e.* the benefits of high energy and high precision [3,4,8–11]. Thus, the proposal for a high-energy muon collider by

* Corresponding author.
E-mail addresses: niveditag@iisc.ac.in (N. Ghosh), skrai@hri.res.in (S.K. Rai), tousik.pdf@iiserkol.ac.in (T. Samui).

https://doi.org/10.1016/j.nuclphysb.2024.116564
Received 10 January 2024; Received in revised form 9 May 2024; Accepted 11 May 2024

Available online 15 May 2024
0550-3213/© 2024 The Author(s). Published by Elsevier B.V. Funded by SCOAP³. This is an open access article under the CC BY license (http://creativecommons.org/licenses/by/4.0/).

the International Muon Collider Collaboration (IMCC) is an important development and a recent growing interest in collider physics [12–15].

The muon collider will mark a new frontier in collider physics, with high luminosity and beam intensity, including 1 ab^{-1} for a 3 TeV machine and 10 ab^{-1} for a 10 TeV machine [3,8]. Its uniqueness lies in the muon beams themselves and it will be the first time in human history that a particle collider will be built with a second-generation particle. Therefore, it offers opportunities to directly study muon-related physics [16–22]. The potential of physics searches of the proposed muon collider has been explored over the last few years. In most studies, the investigations were primarily aimed at the center of mass energy of 10 TeV or more [14]. Furthermore, one expects that the integrated luminosity achievable in this 3 TeV machine will be nearly 1 ab^{-1}, comparable to the luminosity achievable at the 14 TeV LHC. Therefore, the early stages of the muon collider could prove crucial in identifying new physics signals that LHC might not be able to probe even with its high luminosity option.

The broad classes of physics studies at the muon collider consist of precision measurement of electroweak interactions [23–25], Higgs properties [17,19,20,26–30], exploration of new physics sensitivity via higher dimensional effective operators [31], and new physics searches for well-motivated models beyond the SM (BSM) [32–43]. The 'muon-specific' BSM models have an additional advantage in the muon collider [44,45] as they would lead to direct interactions of the new physics sector with the primary colliding beams. The 'muon-philic' (μ-philic) BSM models have been of wide interest, primarily because of the observed excess in the anomalous magnetic moment of the muon, namely $(g-2)_\mu$ [18]. The latest measurement by the 'MUON G-2' collaboration at Fermi National Laboratory (FNAL) combined with the E989 experiment at the Brookhaven National Laboratory (BNL) stands at 5.1σ from its prediction by the Standard Model.[1] In addition, one can also contemplate scenarios where non-trivial physics may be lurking at electroweak energies. These scenarios are likely to stay hidden because they do not interact with the first generation of the SM fermions which have made up almost all the high energy collider primary beams. The proposed muon collider can be a perfect opportunity to search for such μ-philic models.

In this work, we study a new physics scenario containing a leptoquark, a real scalar, and a pair of vector-like leptons (VLL) in the context of a 3 TeV muon collider. This model was proposed to address various flavor anomalies in the quark sector. Its phenomenological implications and collider studies have been discussed in Refs. [62–65]. The model gives rise to non-universal couplings for different generations of leptons (quarks) to the VLLs and real scalar (leptoquark). With an appropriate choice, these non-universal couplings help in explaining the excess in both the quark flavor violation [66–70] and muon magnetic moment, while the lepton flavor violating (LFV) processes remain within the existing experimental bounds. We note that interesting phenomenological studies may exist when the model contains vector-like quarks in addition to VLLs [71–74]. We however restrict ourselves to a model containing only VLLs in this work.

We note that there have been recent works on leptoquark [8,75–78] and VLL [41,79] searches in a muon collider. In our study, we perform a search for leptoquarks in the $2\mu + 2b + \not{E}_T$ final state, extending our earlier study in the context of LHC in Ref. [64], where we mainly focused on the sub-TeV masses of the leptoquark, as LHC is not very sensitive to heavier masses. However, due to the μ-philic nature of the model and the absence of a huge QCD background, a better opportunity to search for such a scenario is easier in the muon collider. In this work, we show that the signature of this model in the same channel for leptoquark mass of around 2 TeV is within the discovery range with just a few fb^{-1} of integrated luminosity at the 3 TeV muon collider.[2] However, as the mass of the leptoquark approaches the kinematic threshold of the collider, it will be difficult to carry out the search and require a higher center of mass energy at the muon collider.

The paper is organized as follows. In section 2, we briefly discuss the model we study in this work. In section 3, we examine how the theoretical and experimental constraints affect our model parameter space. In section 4, we discuss the possibility of probing the leptoquark at a 3 TeV muon collider and finally summarize and conclude in section 5.

2. Model

The model is an extension of the SM particle content where we add new particles, namely, a real scalar (S), a pair of vector-like leptons (ℓ_{4L}, ℓ_{4R}), and a scalar leptoquark (Φ). The only new symmetry introduced beyond the SM gauge symmetry is an additional $\mathbb{Z}_2$ symmetry with an odd charge to all the new particles.

Under this new gauge group symmetry of $\mathcal{G} = SU(3)_C \times SU(2)_L \times U(1)_Y \times \mathbb{Z}_2$, the transformation properties and charges of the new fields are given in Table 1.

The gauge invariant Lagrangian density for the new fields and their interaction with the SM fields is given by

$$\begin{aligned}\mathcal{L} \supset & -\mu_\Phi^2 \Phi^\dagger\Phi - \mu_S^2 S^2 - \lambda_{H\Phi} H^\dagger H \Phi^\dagger\Phi - \lambda_{S\Phi}\Phi^\dagger\Phi S^2 - \lambda_{HS} H^\dagger H S^2 - \lambda_\Phi \left(\Phi^\dagger\Phi\right)^2 - \lambda_S S^4 \\ & - \left\{ h_i \bar{L}_{4R} Q_{Li} \Phi^\dagger + h'_j \bar{L}_{4R} L_{Lj} S + M_F \bar{L}_{4L} L_{4R} + h.c. \right\}, \end{aligned} \tag{1}$$

[1] The 5.1σ excess appears in the measured $(g-2)_\mu$ [46,47] if we consider the presently available consensus SM prediction given in Ref. [48]. However, there are tensions in the Hadronic Vacuum Polarization (HVP) [49–55] contribution to the $(g-2)$ due to the recent lattice QCD based results [56–60] from BMW collaboration and the $e^+e^- \to \pi^+\pi^-$ data from CMD-3 experiment [61].

[2] We can safely assume that with the full 1 ab^{-1} integrated luminosity available, the muon collider will clearly outperform the LHC and leptoquarks with mass of upto 2 TeV will be discovered in our model if we search in the $2\mu + 2b + \not{E}_T$ channel.

Table 1
Charges of the new fields under the gauge group $\mathcal{G}$. All SM particles are even under $\mathbb{Z}_2$.

Particles	$SU(3)_C$	$SU(2)_L$	$U(1)_Y$	$\mathbb{Z}_2$
Φ	3	1	2/3	−1
L_{4L}	1	2	−1/2	−1
L_{4R}	1	2	−1/2	−1
S	1	1	0	−1

where the SM Higgs doublet, quarks, and leptons are represented by H, Q_{Li}, and L_{Lj} $(i,j=1,2,3)$, respectively. The VLL doublet $L_4=(\nu_4,\ell_4^-)^T$ consists of the neutral component ν_4 and charged component ℓ_4^-. The couplings h_i and h'_j are responsible for the new interactions between leptoquark-VLL and VLL-real scalar sector.

The introduction of new neutral scalars generally affects the properties of the SM Higgs boson through mixing with these additional scalars. However, the mixing will be prohibited due to the unbroken $\mathbb{Z}_2$ symmetry in the new sector, as it prevents all such mixing terms at the tree level. This is due to the fact that the new real scalar S is forbidden from getting vacuum expectation value (vev) owing to its $\mathbb{Z}_2$ odd nature. So, the SM Higgs boson becomes massive after the spontaneous breaking of the electroweak symmetry. The masses of Φ and S on the other hand get additional contributions proportional to the electroweak vev which shifts their masses from μ_Φ and $\sqrt{2}\mu_S$ by the $\lambda_{H\Phi}$ and λ_{HS} terms, respectively. The masses then become

$$M_\Phi=\sqrt{\mu_\Phi^2+\frac{\lambda_{H\Phi}v^2}{2}},\qquad \text{and}\quad M_S=\sqrt{2\mu_S^2+\lambda_{HS}v^2}, \tag{2}$$

where v is the vev of the SM Higgs doublet.

Furthermore, the couplings of the SM Higgs boson with the other SM particles remain unchanged at the tree level. Additionally, the new particles are kept heavier than the SM Higgs boson in order to prevent the decay of the Higgs boson to any new modes.

All new contributions to the interaction terms of the SM particles come at the loop level. Note that the leptoquark (Φ) carries a non-zero hypercharge Y as well as color charge and will contribute to both the hgg and $h\gamma\gamma$ couplings at one loop. This change in coupling affects the Higgs signal strength [80]. However, the contributions to the Higgs signal strength in the gluon-gluon fusion production mode and $\gamma\gamma$ decay channel are suppressed and are well within the 2σ limit, provided we keep the leptoquark mass sufficiently heavy [64].

The leptoquark and VLL also interact at the tree level with the SM fermions through the h_i and h'_j couplings. These two sets of couplings are crucial in addressing the excess observed in the experiments and affect the lepton and quark sector properties through the mediation of the new particles in the loop. These two couplings h_i and h'_j get modified after the mixing of quarks and leptons via Cabibbo-Kobayashi-Maskawa (CKM) and Pontecorvo–Maki–Nakagawa–Sakata (PMNS) mixing matrices, respectively. The couplings of the leptoquarks and VLL's with the SM fermions in the physical (mass) basis become

$$h_i^{\rm ph}=\sum_{m=1}^{3}h_m U^d_{mi}\qquad\text{and}\qquad h_i'^{\rm ph}=\sum_{n=1}^{3}h'_n U^\ell_{ni}, \tag{3}$$

where U^d and U^ℓ are the unitary mixing matrices of down-type quarks and leptons, respectively. Non-observation of any significant anomaly in the K^0-$\overline{K^0}$ and B^0-$\overline{B^0}$ oscillations put restrictions on the couplings of the first two generations as $h^{\rm ph}_{1,2}\simeq 0$ [63]. On the other hand, the observed mass splitting between the physical states in the B_s^0-$\overline{B_s^0}$ sets a constraint $|h_2^{\rm ph}h_3^{\rm ph}|\lesssim 0.65$ [63,81]. The other coupling $h_3^{\rm ph}$ does not have strong upper bound from experiment and we have kept it below perturbativity limit [63].

One of the central features of this model is that it can account for the observed excess of the anomalous magnetic moment of muon $(g-2)_\mu$. This excess is explained by introducing the VLLs ℓ_4 and the real scalar S at the one-loop. The lepton flavor violation in $\mu\to e\gamma$ and $\tau\to\mu\gamma$ can be kept under control by choosing h'_1 and h'_3 coupling small. The neutral scalar S can be chosen to be the lightest one among all the $\mathbb{Z}_2$-odd particles. Thus, the particle S can act as a dark matter (DM) candidate. The details of the new physics contribution of this model to $(g-2)_\mu$, implications in flavor physics, and DM aspect of the model have already been studied and analyzed in Ref. [64], and this will be briefly discussed in the next section.

3. Theoretical and experimental constraints

We implement the model file in SARAH [82] and SPheno [83] is used to generate the spectrum files. We use SSP [84] for scanning the parameter space. For the scanning, we have varied the masses in the following range:

$$M_\Phi\in[750:3000]\ \text{GeV},\qquad M_{\ell_4}\in[102.6:500]\ \text{GeV},\qquad M_S\in[65:400]\ \text{GeV} \tag{4}$$

The lower bound of 102.6 GeV on the mass of the charged lepton M_{ℓ_4} comes from Large Electron Positron collider (LEP) [85]. As we will be analyzing the signal at 3 TeV muon collider, we have taken the maximum mass of the LQ to be 3 TeV. The scan range of the VLL is taken to be 500 GeV since it is favored by muon anomaly data. We will see this in the next subsection. As we want our

scalar to be a dark matter candidate, for the scan we have taken $M_S < M_{\ell_4}$ and to evade the $h \to$ invisible decay constraints, we have taken the lower bound on scalar mass to be 65 GeV.

3.1. Muon anomaly and lepton flavor violation

In its recent report [46], the 'MUON G-2' collaboration at the Fermilab National Accelerator Laboratory (FNAL) has announced the experimental measurement of muons anomalous magnetic moment [48]. This anomalous part a_μ is defined in terms of the gyromagnetic ratio or Landé g-factor, which is expected to be 2 at the tree level, as $a_\mu \equiv (g-2)/2$. After taking the effects of loop corrections, the value of a_μ in the SM is expected to be more than zero, and its predicted value, calculated in the SM comes out to be [48–56,86–97]

$$a_\mu^{\rm SM} = 116591810(43) \times 10^{-11}. \tag{5}$$

On the other hand, the experimental uncertainty in the measurements has been brought down by the 'MUON G-2' collaboration at FNAL [98–100] and it has improved significantly to almost half of the uncertainty in the prediction from the SM. However, the measured central value of a_μ in its Run-2 plus Run-3 [46] remained almost the same as the Run-1 [99,100]. The new measurement of a_μ reads as [46]

$$a_\mu^{\text{exp-FNAL}} = 116592055(24) \times 10^{-11}. \tag{6}$$

This new measurement from FNAL makes a new combined world average (combination of FNAL [46,100] and older BNL(2006) [101] data) [46]

$$a_\mu^{\text{exp-comb}} = 116592059(22) \times 10^{-11}. \tag{7}$$

We note here that there are tensions in the SM prediction for the a_μ in Eq. (5) mainly in the hadronic vacuum polarization (HVP) contribution. In the consensus prediction by Ref. [48], the HVP contributions are calculated using experimental e^+e^- annihilation data [49–55]. An alternative *ab initio* calculation using lattice QCD techniques [56–60] for the HVP contribution weakens the tension between the theory prediction and experimental result. Furthermore, the recent $e^+e^- \to \pi^+\pi^-$ result from the CMD-3 experiment [61] disagrees with all previous measurements of this cross-section used in the 2020 White Paper [48] and leads to reduced tension with the experimental result. At present, any firm comparison of the muon $(g-2)$ measurement with the theory is hard to establish and we therefore choose to work in the paradigm that a 5.1σ excess exists, and a contribution from new physics is needed.

In our model, at one-loop, the new physics (NP) contribution to a_μ comes from the scalar S and the VLL and the extra contribution can be expressed as [62,64]

$$\Delta a_\mu = \frac{m_\mu^2 |h_2'|^2}{8\pi^2 M_{\ell_4}^2} f\left(\frac{M_S^2}{M_{\ell_4}^2}\right), \tag{8}$$

where m_μ is the mass of muon and loop function

$$f(x) = \frac{1 - 6x - 6x^2 \ln x + 3x^2 + 2x^3}{12(1-x)^4}. \tag{9}$$

A similar set of Feynman diagrams to muon anomaly will contribute to the LFV process. Non-observation of any significant deviation in the charged lepton sector strongly constrains LFV processes. The strongest bound in the μ–e sector is through the branching ratio of $\mu \to e\gamma$ process from the MEG experiment [102]. Similarly, one also gets constraints from $(\tau \to e\gamma)$ and $(\tau \to \mu\gamma)$ decay branching ratios (BR). The current bounds on these lepton flavor conversions are [103]

$$\text{BR}(\mu \to e\gamma) < 4.2 \times 10^{-13}, \qquad \text{BR}(\tau \to e\gamma) < 3.3 \times 10^{-8}, \qquad \text{BR}(\tau \to \mu\gamma) < 4.4 \times 10^{-8}.$$

We have plotted the allowed parameter space for muon anomaly and LFV in M_S-M_{ℓ_4} and h_2'-M_{ℓ_4} plane in Figs. 1(a) and 1(b), respectively. From the figure, we find that the muon anomaly data favors $M_{\ell_4} \lesssim 330$ GeV and $h_2' \gtrsim 1.5$. The constraints coming from the LFV processes can easily be satisfied by tuning the h_1' and h_3' couplings [64]. We have kept the values of h_1' and h_3' couplings $\mathcal{O}(10^{-5})$ and $\mathcal{O}(10^{-2})$, respectively. Another point worth noticing here is that since the leptoquark is odd under $\mathbb{Z}_2$ and has no direct interaction with any SM lepton (see Eq. (1)), it will not contribute to the muon anomaly and any LFV processes at one loop. It, however, will have a role in quark flavor violation, which puts limits on the leptoquark mass-coupling plane.

3.2. Dark matter

In our model, by virtue of $\mathbb{Z}_2$ symmetry, the lightest BSM particle can act as a DM. In this work, the scalar S is assumed to be the lightest in the BSM sector. This scalar can, therefore, act as a DM candidate. In the present context, we avoid a detailed discussion of the DM aspect of the model. In what follows, we will treat the DM as a type of weakly interacting massive particle (WIMP) that was abundant in the early phase of the universe and was in thermal equilibrium with the other SM particles. As the universe cooled down and expanded, the lighter states did not have sufficient thermal energy to produce the heavier DM particles through interactions,

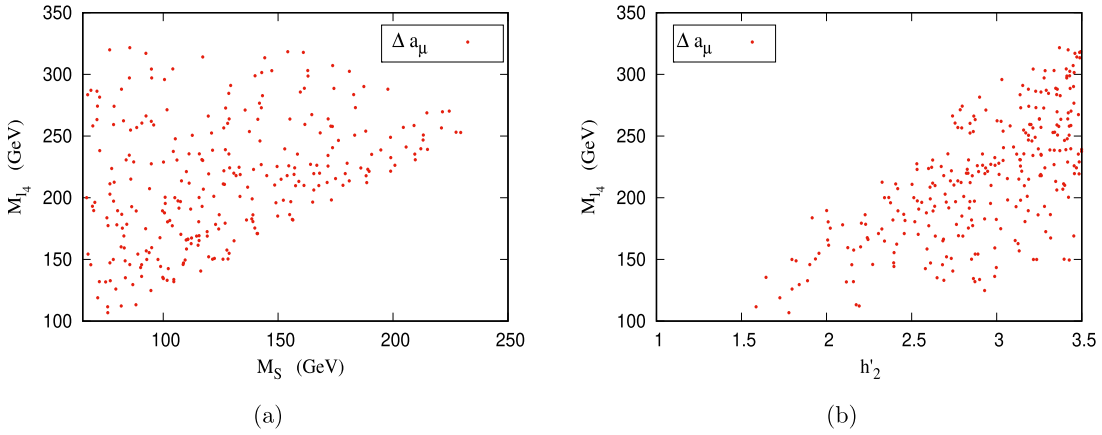

Fig. 1. Parameter space allowed by muon anomaly data in (a) $M_S - M_{\ell_4}$ plane and (b) $h_2' - M_{\ell_4}$ plane. These points also satisfy constraints from LFV measurements. In panel (a), h_2' is varied $\in [1.0, 3.5]$, and, in panel (b), the scan takes $M_S \in [65, 400]$ GeV. So, different points would possibly have different values of h_2' and M_S in panels (a) and (b), respectively.

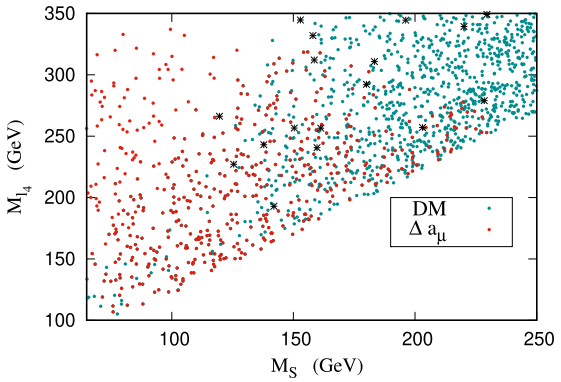

Fig. 2. Parameter space allowed by muon anomaly data at 3σ (red) and DM relic density (blue and black) in M_S-M_{ℓ_4} plane. For DM, relic under-abundant points are represented by blue dots, and the black dots satisfy relic density measurement by PLANCK [104] within 2σ. For the scan, we keep $M_\Phi \in [750 : 3000]$ GeV, $h_2' \in [1.0 : 3.5]$, $h_1' = 10^{-5}$, $h_3' = 10^{-2}$.

and the DM number density became too low to support further interactions and subsequently 'froze out', becoming a persistent relic within the Universe.

The latest measurement of the DM relic density given by Planck [104] is $\Omega_c h^2 = 0.1198 \pm 0.0012$. The other important measurements come from the DM (a) direct detection (DD) and (b) indirect detection experiments. Non-observation of any significant DM signal in any DD experiments puts an upper limit on the DM-nucleon cross-section. For the DM mass range considered in this work, the strongest constraint comes from XENON-1T [105]. On the other hand, the indirect detection experiments constrain the thermally averaged DM annihilation cross-sections $\langle \sigma v \rangle$. For the mass range in our work, the Fermi Large Area Telescope (Fermi-LAT) [106–108] and MAGIC collaboration [109,110] provide an upper limit at 95% C.L. on the DM annihilation cross-section to be $\sim 10^{-25}$ cm^3/s [111] in the $\mu^+\mu^-$ channel.

We have performed a scan to satisfy these DM-related measurements, assuming S as the DM candidate. For the scan, we generated the CALCHEP [112] model file from SARAH [82] and pass it through MICROMEGAS [113], which calculates the DM observables like relic density $\Omega_{\rm DM}h^2$, spin-dependent ($\sigma_{\rm SD}$) and spin-independent ($\sigma_{\rm SI}$) cross-sections, and the thermally averaged annihilation cross-sections ($\langle \sigma v \rangle$). The direct detection constraints are easily satisfied in our model since the scalar S has no direct coupling with the nucleons. On the other hand, in indirect detection, the strongest limits on the parameter are expected from the $\mu^+\mu^-$ channel because of the muon-philic nature of the model. For the parameter range considered in this work, the value of ($\langle \sigma v \rangle$) in this channel lies below the observed value, *i.e.* below 10^{-25} cm^3/s. For the relic density, we require that the DM should not be over-abundant in the present universe, *i.e.* the relic density should be below the observed value by the PLANCK [104]. In Fig. 2, we show the allowed parameter space in M_S - M_{ℓ_4} plane, which satisfies the DM constraints. In the same plane, the allowed point by the muon anomaly data has also been plotted in Fig. 2. We see that smaller mass differences between the DM and VLL are more favored from DM constraints.

Table 2
Benchmark points taken for the collider study and the production cross-section of $\mu^+\mu^- b\bar{b}\not{E}_T$ at 3 TeV muon collider.

	M_Φ (GeV)	M_{ℓ_4} (GeV)	M_S (GeV)	h_2'	$\sigma(\mu^+\mu^- \to \mu^+\mu^- b\bar{b}\not{E}_T)$
BP1	1096.0	182.1	147.0	2.87	28.3 fb
BP2	1621.1	212.8	182.0	2.59	4.5 fb
BP3	1900.2	245.4	199.6	2.88	2.2 fb
BP4	2367.4	258.0	207.5	2.76	0.12 fb

3.3. EW and collider constraints

The high value of h_2' needed for the explanation of the observed excess in the $(g-2)_\mu$ affects the $Z\mu^+\mu^-$ coupling the most. This coupling is measured to be well within SM prediction via electroweak precision observables (EWPO) at the LEP. The deviation allowed for new physics by the EWPO at 2σ is 0.8% [62], *i.e.*

$$\delta g_L^\mu / g_{L,SM}^\mu (M_Z^2) < 0.8\%. \tag{10}$$

The loop diagrams contributing to the g_L^μ coupling are similar to that of the $(g-2)_\mu$ diagrams with the external γ being replaced by Z bosons. The NP contribution can be expressed as

$$\frac{\delta g_L^\mu}{g_{L,\mathrm{SM}}^\mu}(q^2) = \frac{q^2}{32\pi^2 M_{\ell_4}^2} |h_2'|^2 G(x), \tag{11}$$

where $x = \frac{M_S^2}{M_{\ell_4}^2}$ and q is the momentum transfer, i.e. momentum carried by Z boson and

$$G(x) = \frac{7 - 36x + 45x^2 - 16x^3 + (12x^3 - 18x^2)\log x}{36(x-1)^4} \tag{12}$$

For $h_2' = 3.0$ and masses $M_S, M_{\ell_4} > 100$ GeV, the changes are less than 0.3% [64], which is well within the current limit. We have also checked with $h_2' = 3.52$ and have obtained the maximum change to be $\approx 0.4\%$.

The above discussion on the consistency of the parameter space with experimental measurements indicates that the suitable range for relevant parameters could be

$$h_2' \in [1.5, 3.5], \qquad M_\Phi \gtrsim 1000 \text{ GeV}, \qquad M_{l_4} \gtrsim M_S \in [150, 250] \text{ GeV}. \tag{13}$$

With this note, we choose four benchmark points tabulated in Table 2 for our collider studies that will be described in the next section.

4. Collider searches

In this section, we discuss the possibility of producing the leptoquark (Φ) and VLL (ℓ_4) at the muon collider and study the signature of the associated production of these $\mathbb{Z}_2$ odd particles. As opposed to the hadron collider, the pair production of both the leptoquark and VLL at a 3 TeV muon collider will proceed via the photon and Z boson exchange which will have a large s-channel suppression. A more promising channel would be the single production of the leptoquark through the associated production with a VLL and a b quark. This $2 \to 3$ process is found to generate a larger rate of production cross-section and also allows a significantly larger range of leptoquark mass that can be probed since the VLL mass is favored to be lighter than 330 GeV to satisfy the muon anomaly excess. Crucially, this process forces us to involve all the new particles of the model to participate in the interaction which would then require all the new model parameters to be included in the analysis. The VLL decays to a S and a muon and the final decay of the leptoquark gives rise to $2b + 2\mu + \not{E}_T$:

$$\mu^+\mu^- \to \bar{b}\Phi\ell_4^- \to \bar{b}\,(b\ell_4^+)\,(\mu^- S) \to b\bar{b}\mu^+\mu^-\not{E}_T \tag{14}$$

A representative Feynman diagram is depicted in Fig. 3. As the leptoquark is produced in association with the VLL and the production of VLL is proportional to the h_2' coupling, which is large (> 1.5) to satisfy the muon anomaly, it proves to be an advantage for the production cross-section. The muon-philic nature of this model is reflected in the large production of the above-mentioned signal (Table 2). The SM processes that can give rise to similar final states are:

- $\mu^+\mu^- \to \mu^+\mu^- jj\not{E}_T$, where jets are misidentified as b-jet.
- $\mu^+\mu^- \to \mu^+\mu^- b\bar{b}\not{E}_T$ which exactly mimics the signal.

For collider analysis, we have implemented the model file in SARAH [82] and have generated the UFO file to generate signal events at MADGRAPH [114]. The spectrum files for the benchmark points are generated using SPheno [83]. Both the signal and

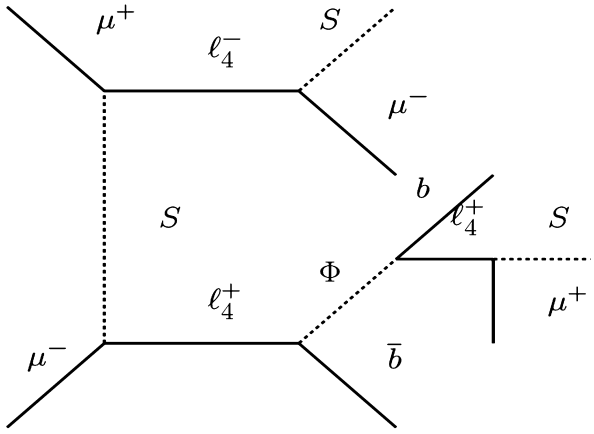

Fig. 3. Representative Feynman Diagram for the process $\mu^+\mu^- \to b\bar{b}\mu^+\mu^- \not{E}_T$.

background events generated in MADGRAPH are passed through PHYTHIA8 [115] for showering and hadronization. Detector simulation is done in DELPHES-3.5.0 [116] by editing the default muon collider card accordingly [117]. For generating SM backgrounds with hard jets, proper MLM matching [118] scheme has been taken into account. We impose the following kinematical acceptance cuts while generating events in MADGRAPH:

$$\begin{aligned} &p_T(j,b) > 20\ \text{GeV}\,; \quad |\eta(j)| < 4.7\,; \quad |\eta(b)| < 2.5\,, \\ &p_T(\ell) > 10\ \text{GeV}\,, \quad |\eta(\ell)| < 2.5\,, \quad \Delta R_{\ell\ell} > 0.4\,, \quad \Delta R_{\ell j} > 0.4\,, \quad \Delta R_{jj} > 0.4\,. \end{aligned} \tag{15}$$

Tagging b-jets in muon collider is not well studied yet as the detector components responsible for measuring impact parameters and displaced vertices are still under research and design. Therefore, we have not used any tagging of the final jets produced at the detector. The jets initiated from the b quarks are treated as normal jets without any b-tagging. The cost we have to pay is that we need to consider the other light quark and gluon-initiated jets, which could be reduced greatly with b-tagging, in the background.

Furthermore, we note that the traditional search for leptoquark in $2\ell + 2j$ channel at the hadron collider [119–123] does not constrain our model much [64]. This is because traditional searches expect low missing energy in the final state, whereas our signal consists of high missing energy. On the other hand, studies prompted by SUSY or VLL searches in the $2\ell + 2b + \not{E}_T$ [124–128] or in the $2\ell + \not{E}_T$ [129–131] channels can, in principle, constrain our model parameters. Although we did not carry out a detailed scan considering these experimental measurements, we have checked that the four benchmark points are not ruled out by any existing analysis in CHECKMATE [132].

We now provide the details of our cut-based analysis. On top of the preselection cuts discussed in Eq. (15), we employ the following selection cuts on the kinematic variables:

- $p_T(\mu)$: We portray the p_T distribution of the leading and sub-leading muons in Fig. 4(a) and Fig. 4(b) respectively. To ensure there are exactly two muons, we put a veto on any third muon with $p_T > 10$ GeV. As we see for backgrounds, the muons tend to populate the higher p_T bins as they come from the hard scattering. We see that $p_T(\mu_1) < 200$ GeV and $p_T(\mu_2) < 100$ GeV helps to reduce the backgrounds.
- $p_T(j)$: Momentum distribution for the leading and sub-leading jets are depicted in Fig. 4(c) and Fig. 4(d). To ensure that the signal contains exactly 2 jets, we reject any third jet with $p_T(j) > 20$ GeV. Compared to the backgrounds, the jets are more boosted for the signal as they come from heavier leptoquark and VLL. Putting cuts of $p_T(j_1) > 250$ GeV and $p_T(j_2) > 150$ GeV helps us to reject the backgrounds drastically.
- $\not{E}_T$: For the signal, the $\not{E}_T$ comes from the scalar mass S (Fig. 4(e)) and hence tends to appear at higher $\not{E}_T$ value. We optimize the cut $\not{E}_T > 100$ GeV to enhance the signal over the background.

We summarize the cut flow effects in Table 3. We calculate the signal significance by using the formula [133]

$$\mathcal{S} = \sqrt{2\left[(S+B)\log\left(\frac{S+B}{B}\right) - S\right]}, \tag{16}$$

where $S(B)$ represents the number of signals (background) events surviving after all the cuts are applied.

We see from Table 3, that the three benchmark points with leptoquark mass < 2 TeV can be probed with 5σ significance with luminosity $< 10\ \text{fb}^{-1}$. However, once the leptoquark mass approaches the kinetic threshold of the muon collider, the signal significance drops significantly and we need higher luminosity to probe the mass of Φ. We also note that the associated production mode allows the probe of the leptoquark with relatively large masses, whereas the pair production would have restricted the search limits to masses $\lesssim \sqrt{s}/2$. A larger center-of-mass energy would further enhance the reach for such leptoquark searches. The DM scalar S also plays a significant role in this search as it mediates the $2 \to 3$ scattering process for leptoquark production. The simultaneous

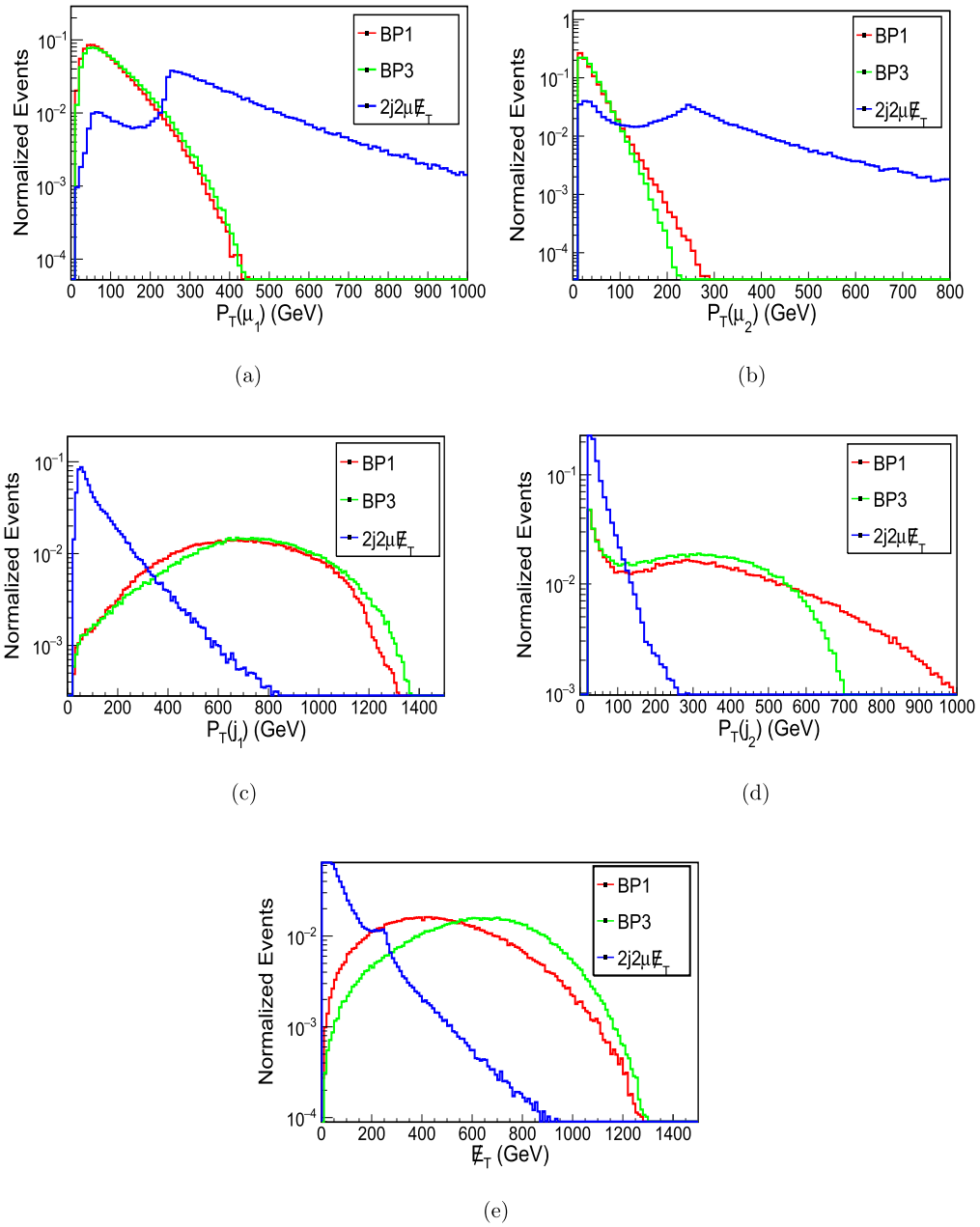

Fig. 4. Normalized distribution of the kinematic variables for the signal and SM backgrounds.

correlation between the flavor sector anomalies and the DM relic abundance also helps in suggesting the regions of parameter space for which this leptoquark production channel is important. We conclude this section with an optimistic outlook, that the muon collider, if built, will be an excellent opportunity to test such μ-philic models of new physics.

5. Conclusion

In this work, we have investigated the potential of a muon collider to search for a model with leptoquark, which carries an odd charge under a discrete $\mathbb{Z}_2$ symmetry. The model we consider in this work extends the SM with a $\mathbb{Z}_2$ symmetry along with a set of particles odd under this new discrete symmetry, *viz.* a VLL, a real scalar, and a leptoquark. The model offers a new physics explanation for the excess seen in the $(g-2)_\mu$ measurement where the new particles contribute to the loops. In this setup, for a substantial parameter space, we see that the muon anomaly is satisfied when the mass of the VLL $M_{\ell_4} < 330$ GeV and $h'_2 > 1.5$. The constraint from LFV measurements is satisfied by keeping h'_1 and h'_3 coupling small. By virtue of the $\mathbb{Z}_2$ symmetry in the BSM sector, the real scalar S can act as a DM, provided the mass difference with VLL is not too large.

Table 3
The cut-flow for signal and backgrounds for $2\mu + 2b + \not{E}_T$ channel at the proposed 3 TeV muon collider and the required luminosity to probe with 5σ significance.

	Number of Events after cuts ($\mathcal{L} = 3000$ fb^{-1})				
SM-background	Preselection	$p_T(\mu)$ cut	$p_T(j)$ cut	$\not{E}_T$ cut	
$\mu^+\mu^- jj$	16376	98	86	38	
$\mu^+\mu^- jj + \not{E}_T$	5285	2296	48	39	
Total background	21661	2394	134	77	
Signal					Luminosity (fb^{-1}) required for 5σ
BP1	29877	26093	19983	19390	0.4
BP2	5061	4595	3447	3396	3.80
BP3	2935	2567	1864	1846	8.7
BP4	146	119	61	61	1950

Guided by the parameter space, which enables us to explain the experimental excesses as well as provide a DM alternative in the theory, we look at the prospect of observing the signatures of these new particles at a muon collider. We identify that the associated production of the $\mathbb{Z}_2$ odd leptoquark with the VLL via the exchange of the DM scalar provides an interesting channel to search for these particles. The proposed search strategy in $2\mu + 2b + \not{E}_T$ offers a significant signal at a 3 TeV muon collider. Discovery of leptoquarks of mass up to 2 TeV can be easily achieved with an integrated luminosity of around 10 fb^{-1} at the 3 TeV machine. This is a significant improvement compared to the LHC, where only a sub-TeV leptoquark could be searched for in the same channel [64]. Due to the phase-space suppression, a 3 TeV muon collider is not suitable for leptoquark search beyond 2 TeV, for which 10 TeV or higher-energy machines will be more useful.

Declaration of competing interest

The authors declare that they have no known competing financial interests or personal relationships that could have appeared to influence the work reported in this paper.

Data availability

No data was used for the research described in the article.

Acknowledgement

The authors acknowledge the support of the Kepler Computing facility maintained by the Department of Physical Sciences, IISER Kolkata, and the RECAPP cluster facility for various computational needs. SKR would like to acknowledge support from the Department of Atomic Energy, Government of India, for the Regional Centre for Accelerator-based Particle Physics (RECAPP). NG would like to thank the IISC-IOE fellowship for financial support. NG would like to thank RECAPP, HRI, Prayagraj for hosting while part of the work was going on. TS would like to thank ICTS, Bengaluru and IISc, Bengaluru for their hospitality during the academic visit.

References

[1] P. Chen, T.L. Barklow, M.E. Peskin, Hadron production in gamma gamma collisions as a background for e+ e- linear colliders, Phys. Rev. D 49 (1994) 3209, arXiv:hep-ph/9305247.
[2] T. Barklow, et al., Beam delivery and beamstrahlung considerations for ultra-high energy linear colliders, arXiv:2305.00573.
[3] T. Han, Y. Ma, K. Xie, High energy leptonic collisions and electroweak parton distribution functions, Phys. Rev. D 103 (2021) L031301, arXiv:2007.14300.
[4] T. Han, Y. Ma, K. Xie, Quark and gluon contents of a lepton at high energies, J. High Energy Phys. 02 (2022) 154, arXiv:2103.09844.
[5] F. Garosi, D. Marzocca, S. Trifinopoulos, LePDF: standard model PDFs for high-energy lepton colliders, J. High Energy Phys. 09 (2023) 107, arXiv:2303.16964.
[6] S. Frixione, G. Stagnitto, The muon parton distribution functions, J. High Energy Phys. 12 (2023) 170, arXiv:2309.07516.
[7] D. Buarque Franzosi, et al., Vector boson scattering processes: status and prospects, Rev. Phys. 8 (2022) 100071, arXiv:2106.01393.
[8] A. Costantini, F. De Lillo, F. Maltoni, L. Mantani, O. Mattelaer, R. Ruiz, et al., Vector boson fusion at multi-TeV muon colliders, J. High Energy Phys. 09 (2020) 080, arXiv:2005.10289.
[9] H. Al Ali, et al., The muon Smasher's guide, Rep. Prog. Phys. 85 (2022) 084201, arXiv:2103.14043.
[10] C. Accettura, et al., Towards a Muon collider, Eur. Phys. J. C 83 (2023) 864, arXiv:2303.08533.
[11] Muon Collider collaboration, The physics case of a 3 TeV muon collider stage, arXiv:2203.07261.
[12] International Muon Collider collaboration, https://muoncollider.web.cern.ch.
[13] D. Schulte, J.-P. Delahaye, M. Diemoz, K. Long, B. Mansoulié, N. Patrone, et al., Muon Collider. A path to the future?, PoS EPS-HEP2019 (2020) 004.
[14] J.P. Delahaye, M. Diemoz, K. Long, B. Mansoulié, N. Pastrone, L. Rivkin, et al., Muon Colliders, arXiv:1901.06150.
[15] International Muon Collider collaboration, The Muon Collider, in: IPAC2022, JACoW, 2022, p. 821.
[16] C.-T. Lu, X. Luo, X. Wei, Exploring muonphilic ALPs at muon colliders, Chin. Phys. C 47 (2023) 103102, arXiv:2303.03110.
[17] T. Han, W. Kilian, N. Kreher, Y. Ma, J. Reuter, T. Striegl, et al., Precision test of the muon-Higgs coupling at a high-energy muon collider, J. High Energy Phys. 12 (2021) 162, arXiv:2108.05362.

[18] R. Dermisek, K. Hermanek, N. McGinnis, Di-Higgs and tri-Higgs boson signals of muon g-2 at a muon collider, Phys. Rev. D 104 (2021) L091301, arXiv:2108.10950.
[19] E. Celada, T. Han, W. Kilian, N. Kreher, Y. Ma, F. Maltoni, et al., Probing Higgs-muon interactions at a multi-TeV muon collider, arXiv:2312.13082.
[20] R. Dermisek, K. Hermanek, T. Lee, N. McGinnis, S. Yoon, Multi Higgs boson signals of a modified muon Yukawa coupling at a muon collider, arXiv:2311.05078.
[21] C. Aime, et al., Muon Collider Physics Summary, arXiv:2203.07256.
[22] K.M. Black, et al., Muon collider forum report, arXiv:2209.01318.
[23] N. Chakrabarty, T. Han, Z. Liu, B. Mukhopadhyaya, Radiative return for heavy Higgs boson at a muon collider, Phys. Rev. D 91 (2015) 015008, arXiv:1408.5912.
[24] L. Di Luzio, R. Gröber, G. Panico, Probing new electroweak states via precision measurements at the LHC and future colliders, J. High Energy Phys. 01 (2019) 011, arXiv:1810.10993.
[25] M. Forslund, P. Meade, Precision Higgs width and couplings with a high energy muon collider, arXiv:2308.02633.
[26] T. Han, D. Liu, I. Low, X. Wang, Electroweak couplings of the Higgs boson at a multi-TeV muon collider, Phys. Rev. D 103 (2021) 013002, arXiv:2008.12204.
[27] M. Chiesa, F. Maltoni, L. Mantani, B. Mele, F. Piccinini, X. Zhao, Measuring the quartic Higgs self-coupling at a multi-TeV muon collider, J. High Energy Phys. 09 (2020) 098, arXiv:2003.13628.
[28] P. Bandyopadhyay, A. Costantini, Obscure Higgs boson at colliders, Phys. Rev. D 103 (2021) 015025, arXiv:2010.02597.
[29] M. Forslund, P. Meade, High precision Higgs from high energy muon colliders, J. High Energy Phys. 08 (2022) 185, arXiv:2203.09425.
[30] J. Reuter, T. Han, W. Kilian, N. Kreher, Y. Ma, T. Striegl, et al., Precision test of the muon-Higgs coupling at a high-energy muon collider, PoS ICHEP2022 (2022) 1239, arXiv:2212.01323.
[31] M. Casarsa, M. Fabbrichesi, E. Gabrielli, Monochromatic single photon events at the muon collider, Phys. Rev. D 105 (2022) 075008, arXiv:2111.13220.
[32] W. Yin, M. Yamaguchi, Muon g-2 at a multi-TeV muon collider, Phys. Rev. D 106 (2022) 033007, arXiv:2012.03928.
[33] T. Han, S. Li, S. Su, W. Su, Y. Wu, Heavy Higgs bosons in 2HDM at a muon collider, Phys. Rev. D 104 (2021) 055029, arXiv:2102.08386.
[34] G.-y. Huang, F.S. Queiroz, W. Rodejohann, Gauged $L_\mu - L_\tau$ at a muon collider, Phys. Rev. D 103 (2021) 095005, arXiv:2101.04956.
[35] G.-y. Huang, S. Jana, F.S. Queiroz, W. Rodejohann, Probing the RK(*) anomaly at a muon collider, Phys. Rev. D 105 (2022) 015013, arXiv:2103.01617.
[36] N. Chakrabarty, I. Chakraborty, D.K. Ghosh, G. Saha, Muon $g-2$ and W-mass in a framework of colored scalars: an LHC perspective, arXiv:2212.14458.
[37] B.A. Ouazghour, A. Arhrib, K. Cheung, E.-s. Ghourmin, L. Rahili, Charged Higgs production at the Muon Collider in the 2HDM, arXiv:2308.15664.
[38] M. Belfkir, T.A. Chowdhury, S. Nasri, Doubly-charged scalars of the Minimal Left-Right Symmetric Model at Muon Colliders, arXiv:2307.16111.
[39] J. Sun, F. Huang, X.-G. He, Muon collider signatures for a Z' with a maximal $\mu - \tau$ coupling in $U(1)_{L_\mu - L_\tau}$, arXiv:2307.00531.
[40] S.P. Maharathy, M. Mitra, Type-II see-saw at $\mu^+\mu^-$ collider, arXiv:2304.08732.
[41] Q. Guo, L. Gao, Y. Mao, Q. Li, Search for vector-like leptons at a Muon Collider, arXiv:2304.01885.
[42] A. Jueid, S. Nasri, Lepton portal dark matter at muon colliders: total rates and generic features for phenomenologically viable scenarios, Phys. Rev. D 107 (2023) 115027, arXiv:2301.12524.
[43] T.A. Chowdhury, A. Jueid, S. Nasri, S. Saad, Probing Zee-Babu states at Muon Colliders, arXiv:2306.01255.
[44] G. Krnjaic, G. Marques-Tavares, D. Redigolo, K. Tobioka, Probing muonphilic force carriers and dark matter at kaon factories, Phys. Rev. Lett. 124 (2020) 041802, arXiv:1902.07715.
[45] S. Jana, S. Klett, Muonic force and neutrino non-standard interactions at muon colliders, arXiv:2308.07375.
[46] Muon g-2 collaboration, Measurement of the positive muon anomalous magnetic moment to 0.20 ppm, arXiv:2308.06230.
[47] Muon g-2 collaboration, New results from the Muon g-2 experiment, in: 2023 European Physical Society Conference on High Energy Physics, vol. 11, 2023, arXiv:2311.08282.
[48] T. Aoyama, et al., The anomalous magnetic moment of the muon in the Standard Model, Phys. Rep. 887 (2020) 1, arXiv:2006.04822.
[49] A. Kurz, T. Liu, P. Marquard, M. Steinhauser, Hadronic contribution to the muon anomalous magnetic moment to next-to-next-to-leading order, Phys. Lett. B 734 (2014) 144, arXiv:1403.6400.
[50] M. Davier, A. Hoecker, B. Malaescu, Z. Zhang, Reevaluation of the hadronic vacuum polarisation contributions to the Standard Model predictions of the muon $g-2$ and $\alpha(m_Z^2)$ using newest hadronic cross-section data, Eur. Phys. J. C 77 (2017) 827, arXiv:1706.09436.
[51] A. Keshavarzi, D. Nomura, T. Teubner, Muon $g-2$ and $\alpha(M_Z^2)$: a new data-based analysis, Phys. Rev. D 97 (2018) 114025, arXiv:1802.02995.
[52] G. Colangelo, M. Hoferichter, P. Stoffer, Two-pion contribution to hadronic vacuum polarization, J. High Energy Phys. 02 (2019) 006, arXiv:1810.00007.
[53] M. Hoferichter, B.-L. Hoid, B. Kubis, Three-pion contribution to hadronic vacuum polarization, J. High Energy Phys. 08 (2019) 137, arXiv:1907.01556.
[54] M. Davier, A. Hoecker, B. Malaescu, Z. Zhang, A new evaluation of the hadronic vacuum polarisation contributions to the muon anomalous magnetic moment and to $\boldsymbol{\alpha(m_Z^2)}$, Eur. Phys. J. C 80 (2020) 241, arXiv:1908.00921.
[55] A. Keshavarzi, D. Nomura, T. Teubner, The $g-2$ of charged leptons, $\alpha(M_Z^2)$ and the hyperfine splitting of muonium, Phys. Rev. D 101 (2020) 014029, arXiv:1911.00367.
[56] T. Blum, N. Christ, M. Hayakawa, T. Izubuchi, L. Jin, C. Jung, et al., The hadronic light-by-light scattering contribution to the muon anomalous magnetic moment from lattice QCD, Phys. Rev. Lett. 124 (2020) 132002, arXiv:1911.08123.
[57] S. Borsanyi, et al., Leading hadronic contribution to the muon magnetic moment from lattice QCD, Nature 593 (2021) 51, arXiv:2002.12347.
[58] M. Cè, et al., Window observable for the hadronic vacuum polarization contribution to the muon g-2 from lattice QCD, Phys. Rev. D 106 (2022) 114502, arXiv:2206.06582.
[59] Extended Twisted Mass Collaboration, Lattice Calculation of the Short and Intermediate Time-Distance Hadronic Vacuum Polarization Contributions to the Muon Magnetic Moment Using Twisted-Mass Fermions, Phys. Rev. D 107 (2023) 074506, arXiv:2206.15084.
[60] E.-H. Chao, H.B. Meyer, J. Parrino, Coordinate-space calculation of the window observable for the hadronic vacuum polarization contribution to (g-2)μ, Phys. Rev. D 107 (2023) 054505, arXiv:2211.15581.
[61] CMD-3 collaboration, Measurement of the $e^+e^- \to \pi^+\pi^-$ cross section from threshold to 1.2 GeV with the CMD-3 detector, arXiv:2302.08834.
[62] P. Arnan, L. Hofer, F. Mescia, A. Crivellin, Loop effects of heavy new scalars and fermions in $b \to s\mu^+\mu^-$, J. High Energy Phys. 04 (2017) 043, arXiv:1608.07832.
[63] L. Dhargyal, S.K. Rai, Implications of a vector-like lepton doublet and scalar Leptoquark on $R(D^{(*)})$, arXiv:1806.01178.
[64] N. Ghosh, S.K. Rai, T. Samui, Collider signatures of a scalar leptoquark and vectorlike lepton in light of muon anomaly, Phys. Rev. D 107 (2023) 035028, arXiv:2206.11718.
[65] K. Cheung, T.T.Q. Nguyen, C.J. Ouseph, Leptoquark search at the Forward Physics Facility, Phys. Rev. D 108 (2023) 036014, arXiv:2302.05461.
[66] Heavy Flavor Averaging Group (HFAG) collaboration, Averages of b-hadron, c-hadron, and τ-lepton properties as of summer 2014, arXiv:1412.7515.
[67] M. Misiak, et al., Updated NNLO QCD predictions for the weak radiative B-meson decays, Phys. Rev. Lett. 114 (2015) 221801, arXiv:1503.01789.
[68] Fermilab Lattice, MILC collaboration, $B^0_{(s)}$-mixing matrix elements from lattice QCD for the Standard Model and beyond, Phys. Rev. D 93 (2016) 113016, arXiv:1602.03560.
[69] HFLAV collaboration, Averages of b-hadron, c-hadron, and τ-lepton properties as of 2021, Phys. Rev. D 107 (2023) 052008, arXiv:2206.07501.
[70] LHCb collaboration, Measurement of lepton universality parameters in $B^+ \to K^+\ell^+\ell^-$ and $B^0 \to K^{*0}\ell^+\ell^-$ decays, Phys. Rev. D 108 (2023) 032002, arXiv:2212.09153.
[71] H.-J. He, T.M.P. Tait, C.P. Yuan, New top flavor models with seesaw mechanism, Phys. Rev. D 62 (2000) 011702, arXiv:hep-ph/9911266.
[72] H.-J. He, C.T. Hill, T.M.P. Tait, Top quark seesaw, vacuum structure and electroweak precision constraints, Phys. Rev. D 65 (2002) 055006, arXiv:hep-ph/0108041.

[73] X.-F. Wang, C. Du, H.-J. He, LHC Higgs signatures from topflavor seesaw mechanism, Phys. Lett. B 723 (2013) 314, arXiv:1304.2257.
[74] H.-J. He, Z.-Z. Xianyu, Extending Higgs inflation with TeV scale new physics, J. Cosmol. Astropart. Phys. 10 (2014) 019, arXiv:1405.7331.
[75] P. Asadi, R. Capdevilla, C. Cesarotti, S. Homiller, Searching for leptoquarks at future muon colliders, J. High Energy Phys. 10 (2021) 182, arXiv:2104.05720.
[76] P. Bandyopadhyay, A. Karan, R. Mandal, S. Parashar, Distinguishing signatures of scalar leptoquarks at hadron and muon colliders, Eur. Phys. J. C 82 (2022) 916, arXiv:2108.06506.
[77] S. Qian, C. Li, Q. Li, F. Meng, J. Xiao, T. Yang, et al., Searching for heavy leptoquarks at a muon collider, J. High Energy Phys. 12 (2021) 047, arXiv:2109.01265.
[78] N. Desai, A. Sengupta, Status of leptoquark models after LHC Run-2 and discovery prospects at future colliders, arXiv:2301.01754.
[79] A.P. Morais, A. Onofre, F.F. Freitas, J.a. Gonçalves, R. Pasechnik, R. Santos, Deep learning searches for vector-like leptons at the LHC and electron/muon colliders, Eur. Phys. J. C 83 (2023) 232, arXiv:2108.03926.
[80] CMS collaboration, A portrait of the Higgs boson by the CMS experiment ten years after the discovery, Nature 607 (2022) 60, arXiv:2207.00043.
[81] L. Di Luzio, M. Kirk, A. Lenz, Updated B_s-mixing constraints on new physics models for $b \to s\ell^+\ell^-$ anomalies, Phys. Rev. D 97 (2018) 095035, arXiv:1712.06572.
[82] F. Staub, SARAH, arXiv:0806.0538.
[83] W. Porod, F. Staub, SPheno 3.1: extensions including flavour, CP-phases and models beyond the MSSM, Comput. Phys. Commun. 183 (2012) 2458, arXiv:1104.1573.
[84] F. Staub, T. Ohl, W. Porod, C. Speckner, A tool box for implementing supersymmetric models, Comput. Phys. Commun. 183 (2012) 2165, arXiv:1109.5147.
[85] Particle Data Group collaboration, Review of particle physics, PTEP 2022 (2022) 083C01.
[86] T. Aoyama, M. Hayakawa, T. Kinoshita, M. Nio, Complete tenth-order QED contribution to the muon $g-2$, Phys. Rev. Lett. 109 (2012) 111808, arXiv:1205.5370.
[87] T. Aoyama, T. Kinoshita, M. Nio, Theory of the anomalous magnetic moment of the electron, Atoms 7 (2019) 28.
[88] A. Czarnecki, W.J. Marciano, A. Vainshtein, Refinements in electroweak contributions to the muon anomalous magnetic moment, Phys. Rev. D 67 (2003) 073006, arXiv:hep-ph/0212229.
[89] C. Gnendiger, D. Stöckinger, H. Stöckinger-Kim, The electroweak contributions to $(g-2)_\mu$ after the Higgs boson mass measurement, Phys. Rev. D 88 (2013) 053005, arXiv:1306.5546.
[90] K. Melnikov, A. Vainshtein, Hadronic light-by-light scattering contribution to the muon anomalous magnetic moment revisited, Phys. Rev. D 70 (2004) 113006, arXiv:hep-ph/0312226.
[91] P. Masjuan, P. Sánchez-Puertas, Pseudoscalar-pole contribution to the $(g_\mu - 2)$: a rational approach, Phys. Rev. D 95 (2017) 054026, arXiv:1701.05829.
[92] G. Colangelo, M. Hoferichter, M. Procura, P. Stoffer, Dispersion relation for hadronic light-by-light scattering: two-pion contributions, J. High Energy Phys. 04 (2017) 161, arXiv:1702.07347.
[93] M. Hoferichter, B.-L. Hoid, B. Kubis, S. Leupold, S.P. Schneider, Dispersion relation for hadronic light-by-light scattering: pion pole, J. High Energy Phys. 10 (2018) 141, arXiv:1808.04823.
[94] A. Gérardin, H.B. Meyer, A. Nyffeler, Lattice calculation of the pion transition form factor with $N_f = 2+1$ Wilson quarks, Phys. Rev. D 100 (2019) 034520, arXiv:1903.09471.
[95] J. Bijnens, N. Hermansson-Truedsson, A. Rodríguez-Sánchez, Short-distance constraints for the HLbL contribution to the muon anomalous magnetic moment, Phys. Lett. B 798 (2019) 134994, arXiv:1908.03331.
[96] G. Colangelo, F. Hagelstein, M. Hoferichter, L. Laub, P. Stoffer, Longitudinal short-distance constraints for the hadronic light-by-light contribution to $(g-2)_\mu$ with large-N_c Regge models, J. High Energy Phys. 03 (2020) 101, arXiv:1910.13432.
[97] G. Colangelo, M. Hoferichter, A. Nyffeler, M. Passera, P. Stoffer, Remarks on higher-order hadronic corrections to the muon $g-2$, Phys. Lett. B 735 (2014) 90, arXiv:1403.7512.
[98] Muon g-2 collaboration, Muon (g-2) technical design report, arXiv:1501.06858.
[99] Muon g-2 collaboration, Measurement of the anomalous precession frequency of the muon in the Fermilab Muon $g-2$ experiment, Phys. Rev. D 103 (2021) 072002, arXiv:2104.03247.
[100] Muon g-2 collaboration, Measurement of the positive muon anomalous magnetic moment to 0.46 ppm, Phys. Rev. Lett. 126 (2021) 141801, arXiv:2104.03281.
[101] Muon g-2 collaboration, Final report of the muon E821 anomalous magnetic moment measurement at BNL, Phys. Rev. D 73 (2006) 072003, arXiv:hep-ex/0602035.
[102] MEG collaboration, Search for the lepton flavour violating decay $\mu^+ \to e^+\gamma$ with the full dataset of the MEG experiment, Eur. Phys. J. C 76 (2016) 434, arXiv:1605.05081.
[103] BaBar collaboration, Searches for lepton flavor violation in the decays $\tau^\pm \to e^\pm\gamma$ and $\tau^\pm \to \mu^\pm\gamma$, Phys. Rev. Lett. 104 (2010) 021802, arXiv:0908.2381.
[104] Planck collaboration, Planck 2018 results. VI. Cosmological parameters, Astron. Astrophys. 641 (2020) A6, arXiv:1807.06209.
[105] XENON collaboration, Dark matter search results from a one ton-year exposure of XENON1T, Phys. Rev. Lett. 121 (2018) 111302, arXiv:1805.12562.
[106] Fermi-LAT collaboration, Dark matter constraints from observations of 25 Milky Way satellite galaxies with the Fermi Large Area Telescope, Phys. Rev. D 89 (2014) 042001, arXiv:1310.0828.
[107] Fermi-LAT collaboration, Searching for dark matter annihilation from Milky Way dwarf spheroidal galaxies with six years of Fermi Large Area Telescope data, Phys. Rev. Lett. 115 (2015) 231301, arXiv:1503.02641.
[108] Fermi-LAT, DES collaboration, Searching for dark matter annihilation in recently discovered Milky Way satellites with Fermi-LAT, Astrophys. J. 834 (2017) 110, arXiv:1611.03184.
[109] MAGIC collaboration, Searches for Dark Matter annihilation signatures in the Segue 1 satellite galaxy with the MAGIC-I telescope, J. Cosmol. Astropart. Phys. 06 (2011) 035, arXiv:1103.0477.
[110] J. Aleksić, et al., Optimized dark matter searches in deep observations of Segue 1 with MAGIC, J. Cosmol. Astropart. Phys. 02 (2014) 008, arXiv:1312.1535.
[111] MAGIC, Fermi-LAT collaboration, Limits to dark matter annihilation cross-section from a combined analysis of MAGIC and Fermi-LAT observations of dwarf satellite galaxies, J. Cosmol. Astropart. Phys. 02 (2016) 039, arXiv:1601.06590.
[112] A. Belyaev, N.D. Christensen, A. Pukhov, CalcHEP 3.4 for collider physics within and beyond the Standard Model, Comput. Phys. Commun. 184 (2013) 1729, arXiv:1207.6082.
[113] G. Bélanger, F. Boudjema, A. Pukhov, A. Semenov, micrOMEGAs4.1: two dark matter candidates, Comput. Phys. Commun. 192 (2015) 322, arXiv:1407.6129.
[114] J. Alwall, R. Frederix, S. Frixione, V. Hirschi, F. Maltoni, O. Mattelaer, et al., The automated computation of tree-level and next-to-leading order differential cross sections, and their matching to parton shower simulations, J. High Energy Phys. 07 (2014) 079, arXiv:1405.0301.
[115] T. Sjöstrand, S. Ask, J.R. Christiansen, R. Corke, N. Desai, P. Ilten, et al., An introduction to PYTHIA 8.2, Comput. Phys. Commun. 191 (2015) 159, arXiv:1410.3012.
[116] DELPHES 3 collaboration, DELPHES 3, a modular framework for fast simulation of a generic collider experiment, J. High Energy Phys. 02 (2014) 057, arXiv:1307.6346.
[117] CERN collaboration, Talk: Delphes card for muon collider.
[118] S. Hoeche, F. Krauss, N. Lavesson, L. Lonnblad, M. Mangano, A. Schalicke, et al., Matching parton showers and matrix elements, in: HERA and the LHC: A Workshop on the Implications of HERA for LHC Physics: CERN - DESY Workshop 2004/2005, Midterm Meeting, CERN, 11-13 October 2004; Final Meeting, DESY, 17-21 January 2005, 2005, pp. 288–289, arXiv:hep-ph/0602031.

[119] D0 collaboration, Search for scalar leptoquarks in the acoplanar jet topology in $p\bar{p}$ collisions at $\sqrt{s}$ = 1.96-TeV, Phys. Lett. B 640 (2006) 230, arXiv:hep-ex/0607009.
[120] ATLAS collaboration, Search for pairs of scalar leptoquarks decaying into quarks and electrons or muons in $\sqrt{s}$ = 13 TeV pp collisions with the ATLAS detector, J. High Energy Phys. 10 (2020) 112, arXiv:2006.05872.
[121] ATLAS collaboration, Search for pair production of third-generation leptoquarks decaying into a bottom quark and a τ-lepton with the ATLAS detector, arXiv:2303.01294.
[122] ATLAS collaboration, Search for excited τ-leptons and leptoquarks in the final state with τ-leptons and jets in pp collisions at $\sqrt{s}$ = 13 TeV with the ATLAS detector, J. High Energy Phys. 06 (2023) 199, arXiv:2303.09444.
[123] CMS collaboration, Search for a third-generation leptoquark coupled to a τ lepton and a b quark through single, pair, and nonresonant production in proton-proton collisions at $\sqrt{s}$ = 13 TeV, arXiv:2308.07826.
[124] ATLAS collaboration, Search for top squarks in final states with one isolated lepton, jets, and missing transverse momentum in $\sqrt{s}$ = 13 TeV pp collisions with the ATLAS detector, ATLAS-CONF-2016-050.
[125] ATLAS collaboration, Search for squarks and gluinos in events with an isolated lepton, jets and missing transverse momentum at $\sqrt{s}$ = 13 TeV with the ATLAS detector, ATLAS-CONF-2016-054.
[126] ATLAS collaboration, Search for direct top squark pair production and dark matter production in final states with two leptons in $\sqrt{s}$ = 13 TeV pp collisions using 13.3 fb^{-1} of ATLAS data, ATLAS-CONF-2016-076.
[127] ATLAS collaboration, Search for a scalar partner of the top quark in the jets plus missing transverse momentum final state at $\sqrt{s}$ = 13 TeV with the ATLAS detector, J. High Energy Phys. 12 (2017) 085, arXiv:1709.04183.
[128] ATLAS collaboration, Search for squarks and gluinos in final states with jets and missing transverse momentum using 36 fb^{-1} of $\sqrt{s}$ = 13 TeV pp collision data with the ATLAS detector, Phys. Rev. D 97 (2018) 112001, arXiv:1712.02332.
[129] ATLAS collaboration, Search for electroweak production of supersymmetric states in scenarios with compressed mass spectra at $\sqrt{s}$ = 13 TeV with the ATLAS detector, Phys. Rev. D 97 (2018) 052010, arXiv:1712.08119.
[130] CMS collaboration, Search for new physics in events with two soft oppositely charged leptons and missing transverse momentum in proton-proton collisions at $\sqrt{s}$ = 13 TeV, Phys. Lett. B 782 (2018) 440, arXiv:1801.01846.
[131] ATLAS collaboration, Search for electroweak production of supersymmetric particles in final states with two or three leptons at $\sqrt{s}$ = 13 TeV with the ATLAS detector, Eur. Phys. J. C 78 (2018) 995, arXiv:1803.02762.
[132] M. Drees, H. Dreiner, D. Schmeier, J. Tattersall, J.S. Kim, CheckMATE: confronting your favourite new physics model with LHC data, Comput. Phys. Commun. 187 (2015) 227, arXiv:1312.2591.
[133] G. Cowan, K. Cranmer, E. Gross, O. Vitells, Asymptotic formulae for likelihood-based tests of new physics, Eur. Phys. J. C 71 (2011) 1554, arXiv:1007.1727.